Materials Letters 232 (2018) 179–182

Contents lists available at ScienceDirect

Materials Letters

journal homepage: www.elsevier.com/locate/mlblue

In situ formation of metal matrix composites using binder jet additive manufacturing (3D printing)

Pablo D. Enrique *, Yahya Mahmoodkhani, Ehsan Marzbanrad, Ehsan Toyserkani, Norman Y. Zhou

University of Waterloo, 200 University Ave W, Waterloo, Ontario N2L 3G1, Canada

ARTICLE INFO

Article history:
Received 14 July 2018
Received in revised form 20 August 2018
Accepted 21 August 2018
Available online 23 August 2018

Keywords:
Binder jet additive manufacturing
Metal matrix composite
Inconel 625
Cermet
Microstructure
Sintering

ABSTRACT

Simplifying the manufacturing of metal matrix composites (MMCs) will allow for their wider use in applications that require lower density, higher strength, and high wear resistance when compared to traditional metals. An in-situ method of MMC formation is proposed, using a binder jet additive manufacturing (BJ-AM) process with only Inconel 625 powder and a carbon-containing binder. Carbide formation occurs at elevated temperatures during sintering by combining Cr, Mo and Nb alloying elements in Inconel 625 and carbon from the binder. The core-shell morphology and composition of the final MMC is tuned by controlling the quantity of carbon in the system during the sintering step.

1. Introduction

In the past, the use of metal matrix composites (MMCs) was limited due to manufacturing challenges. However, their high specific strength, high specific stiffness, high wear resistance and other beneficial properties make them useful in many applications including cutting tools and high temperature components [1–3]. Liquid-state and vapor-state processing often results in inhomogeneous dispersions of the reinforcing phase within the metal matrix. Recent solutions focus on the use of solid-state processing, in which two types of powder particles – the matrix and reinforcing phase – are mixed together and sintered or locally melted [2,4–7]. In this work, the solid-state process is simplified even further; MMCs with Inconel 625 matrix are generated in-situ during binder jet additive manufacturing (BJ-AM), using the high carbon content of the binder and alloying elements within the Inconel 625 powder particles.

2. Material and methods

2.1. Binder jet additive manufacturing

Spherical Inconel 625 powder particles with average particle size of approximately 24 μm were used in the BJ-AM process. BJ-AM was performed with a ZCorp Z 510/310 binder jet 3D printer by 3D SYSTEMS that was modified for small builds. A CAD model of a rectangular shape ($2.5 \times 10 \times 20$ mm) was created and 70 μm layer thickness was considered in the model for layer by layer printing. The feed bed was loaded with Inconel 625, after which a piston was programmed to move the feed bed upwards by one-layer thickness of 70 μm, where a roller spreads the powder onto the build bed. A binder (zb60 by 3D Systems) was applied through a print head at 360 dpi with 7 drop sizes ranging from 6 to 42 pL. A saturation level of 100% and 200% (for the core and shell respectively) was used and the temperature of the part during and after printing was kept at 35 °C for three hours. Once the binder is dry, the green solid part is carefully separated from loose powder and cut in half to facilitate handling. Additional zb60 binder with 3 wt% PVA was added dropwise to the outside of the part to increase the strength and then dried with a 100 W tungsten lamp.

2.2. Post-processing

Green binder jet printed parts were post-processed to increase strength by sintering the powder particles together. For one set of samples, the sintering process included a binder burn-off step during which the binder decomposed, reacted with H_2 gas in the furnace and was partially removed. These samples experienced a 1 h

* Corresponding author.
E-mail address: pdenriqu@uwaterloo.ca (P.D. Enrique).

https://doi.org/10.1016/j.matlet.2018.08.117
0167-577X/

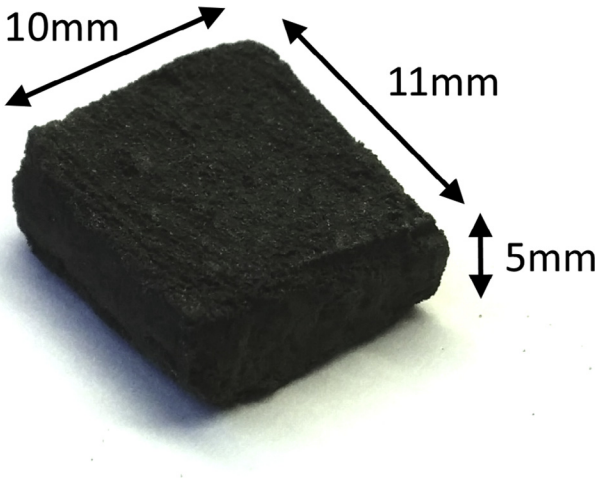

Fig. 1. Dimensions of BJ-AM MMC part after sintering.

hold at 527 °C during which a 5% H_2 atmosphere mixture (argon balance) was used. After the burn-off stage was completed, the atmosphere was switched to high purity argon and the sintering step was performed in this inert environment. The second set of samples did not experience a burn-off step and were sintered directly in high purity argon.

Both sets of samples were post-processed in a horizontal tube furnace with a sintering temperature of 1200 °C. For both sets of samples, the ramp rate when heating the furnace to the burn-off temperature was 3 °C/min and the ramp rate to reach the sintering temperature was 5 °C/min. A holding period of 5 h was used for sintering the parts. At the conclusion of the holding period, the parts were removed from the furnace and air cooled. An example part is shown in Fig. 1.

2.3. Characterization methods

Analysis was performed with a JEOL JSM-6460 scanning electron microscope (SEM) and Oxford Instruments INCAx-sight EDX attachment. GIXRD analysis was performed using a PANalytical X'pert Pro MRD HR-XRD, and etching of Inconel 625 was done by immersion in an inverted glyceregia etchant ($HCl:HNO_3$:Glycerol in a 5:1:1 ratio) for 1.5 min.

3. Results

The use of an inert environment during the burn-off stage of the sintering process results in particles with a Cr_3C_2 shell, as shown in Fig. 2a and identified in an XRD scan in Fig. 3. Performing the burn-off stage in a reducing environment leaves only the core structure, as seen in Fig. 2b. EDX scanning reveals that the outer shell is composed of the Cr-rich phase, whereas the smaller core carbides are Nb-rich and Mo-rich phases (Table 1). These are identified in the XRD scan as NbC and Mo_2C.

Carbides are well known for their corrosion resistance and high hardness, which was made evident in the etched cross-sections. Use of inverted glyceregia as an etchant is found to preferentially attack the sensitized nickel matrix in Fig. 2c, which displays heavy chromium, molybdenum and niobium depletion based on EDX measurements (Table 1). Etched cross-sectional images of the BJ-AM parts show that the blocky Cr_3C_2 and smaller NbC and Mo_2C phases do not only exist at the particle surface but also within the particles.

4. Discussion

Typical carbide phases in solution treated and aged Inconel 625 include Mo_6C and $Cr_{23}C_6$, with some Mo and Cr substitution possible in each phase [8]. Carbon content in traditionally manufactured Inconel 625 is limited to 0.1% and chromium-carbon phase diagrams identify the preferred carbide as $Cr_{23}C_6$ at the sintering process temperature of 1200 °C [9]. However, based on the phase diagram, the presence of an external source that increases the atomic percent of carbon beyond 40% in a chromium-carbon system will result in the formation of Cr_3C_2 carbides and residual carbon. Both of these were detected phases in the XRD analysis. High carbon content binder from the printing process decomposed and remained within the porous structure of the BJ-AM made part, combining with Cr, Nb and Mo alloying elements during sintering and cooling. Since a reduction in carbon content eliminated the presence of the Cr_3C_2 shell, it is expected that the formation of NbC and Mo_2C phases are kinetically favoured.

NiCr-Cr_3C_2 metal matrix composites have been previously investigated in literature. Applied as a coating using high velocity oxygen fuel spraying [10] or laser cladding techniques [11], studies have shown improved wear resistance over uncoated Inconel materials. Bulk NiCr-Cr_3C_2 components have been produced by sintering of Ni, Cr, C and/or Cr_3C_2 powders (or some combination thereof) [4,6,7], with the carbide phase resulting in an increased hardness, and the ductile nickel phase resulting in a higher fracture toughness than can be expected in a pure ceramic component [12]. However, the use of Inconel 625 as the nickel and chromium source, and the binder as a carbon source, may result in different properties. Loss of chromium from the nickel matrix to the Cr_3C_2 phase is expected to result in a higher corrosion rate of the sensitized nickel matrix when compared to the original Inconel 625 [13], however the overall wear resistance is expected to be higher. A partial burn-off step, as is performed for the sample shown in Fig. 2b, forms NbC and Mo_2C phases while preventing the growth of the Cr_3C_2 shell. These samples are expected to demonstrate good wear resistance while also maintaining Inconel 625's oxidation resistance at elevated temperatures, which is attributed to chromium within the nickel matrix forming Cr_2O_3 scales that prevent oxygen diffusion into the bulk of the material [14,15].

5. Conclusion

Metal matrix composites using Inconel 625 powder particles and a carbon-containing binder were fabricated via binder jet additive manufacturing. Variations in sintering condition influenced the morphology of the sintered powder particles:

- The use of an inert atmosphere throughout the sintering process resulted in the formation of a core-shell structure. The shell was composed of a Cr_3C_2 phase, and the core was composed of a nickel matrix with NbC, Mo_2C and Cr_3C_2 phases.
- The use of an argon atmosphere with 5% H_2 during a 1-hour binder burn-off step resulted in a core structure without the presence of the Cr_3C_2 shell. Significant quantities of NbC and Mo_2C phases were still present, suggesting that changes in the carbon quantity remaining after burn-off can be used to modify the morphology, composition and properties of the final metal matrix composite.

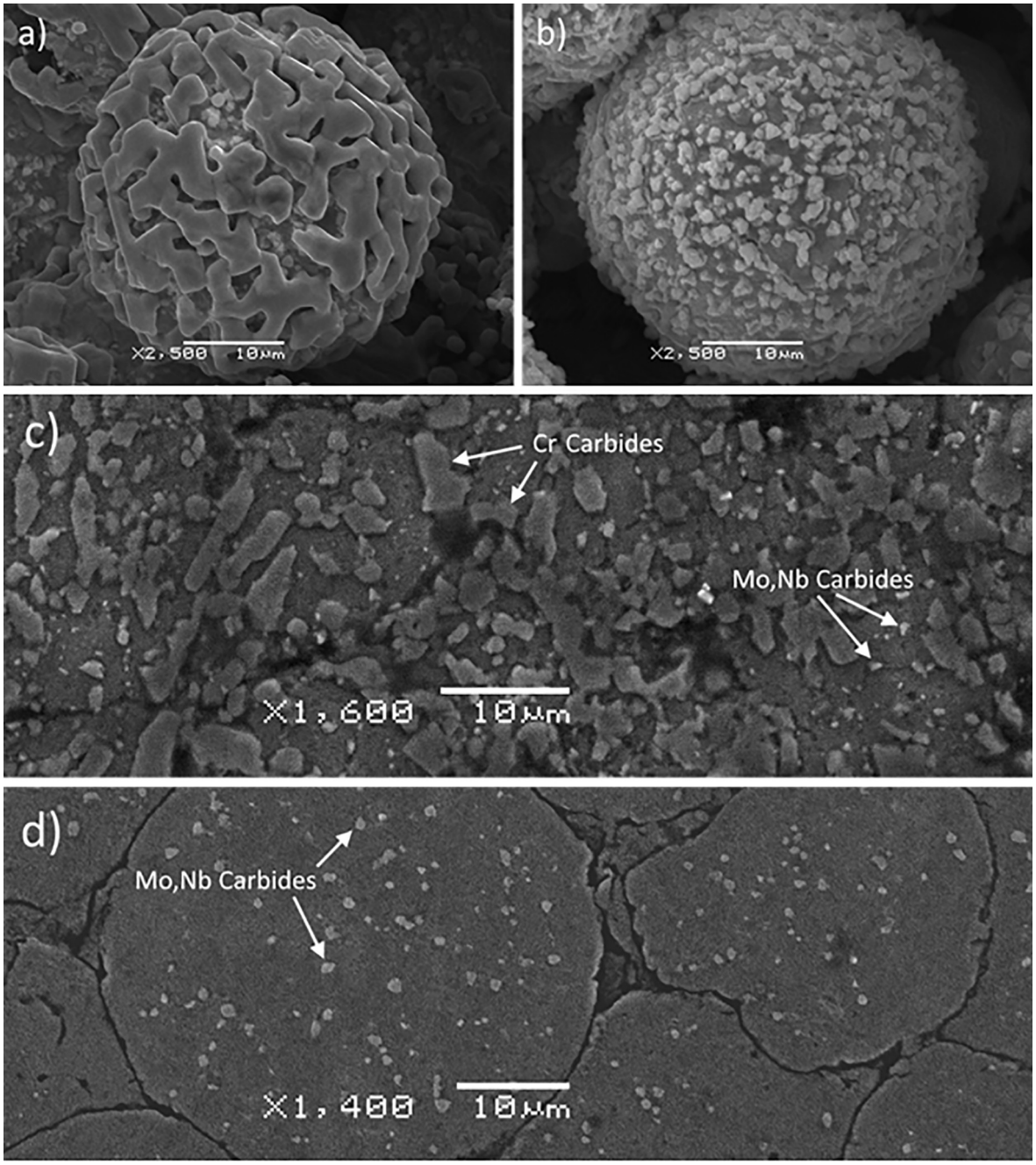

Fig. 2. Microstructure of particles sintered with a) no burn-off step, b) 1 h burn-off step in 5% H_2 and c-d) their respective cross sections after etching.

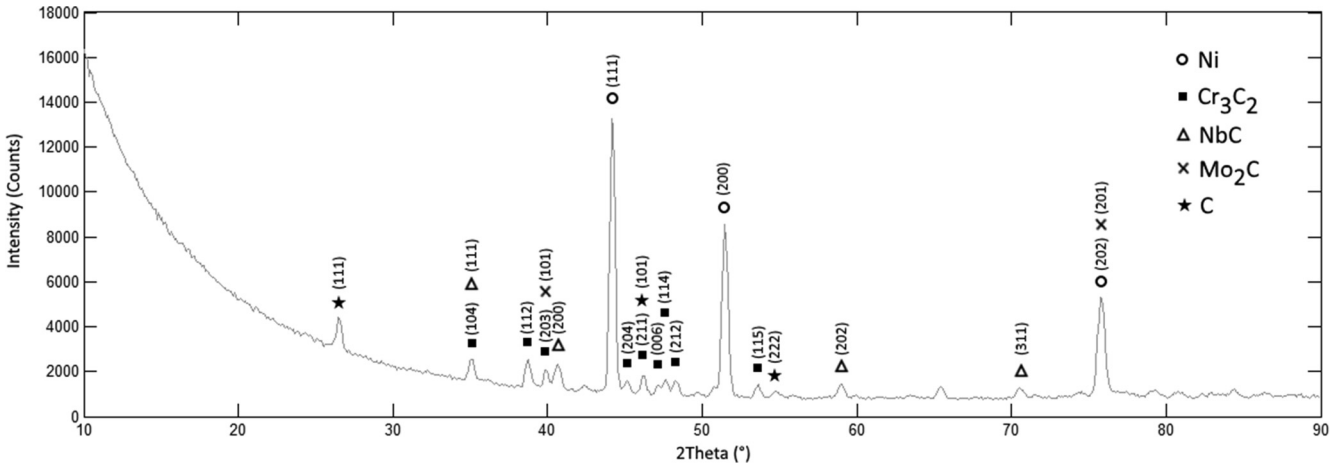

Fig. 3. GIXRD analysis of a BJ-AM part sintered with no burn-off step.

Table 1
EDX composition (wt%) of various phases in as-sintered BJ-AM part with no binder burn-off step.

Phase	Ni	Cr	Mo	Nb	Fe
Cr-rich	5.2	73.5	19.6		1.7
(Mo,Nb)-rich	9.4	23.0	56.3	9.9	1.4
Sensitized Ni Matrix	75.9	9.5	6.7		7.9
Inconel 625	≥58.0	20.0–23.0	8.0–10.0	3.15–4.15	≤5.0

Acknowledgements

This work was performed with funding support from the Natural Sciences and Engineering Research Council of Canada (NSERC) and the Canada Research Chairs (CRC) Program, in collaboration with the Centre for Advanced Materials Joining and the Multi-Scale Additive Manufacturing Lab at the University of Waterloo.

References

[1] S.P. Rawal, Metal-matrix composites for space applications, JOM 53 (2001) 14–17, https://doi.org/10.1007/s11837-001-0139-z.
[2] A.M. Russell, K.L. Lee, Structure-Property Relations in Nonferrous Metals, John Wiley & Sons, 2005.
[3] M. Haghshenas, Metal–matrix composites, Ref. Modul. Mater. Sci. Mater. Eng., Elsevier, 2016, pp. 0–28. doi: 10.1016/B978-0-12-803581-8.03950-3.
[4] W. Zhai, Y. Gao, L. Sun, Y. Wang, K. Niwa, M. Hasegawa, High pressure in-situ synthesis and physical properties of Cr3C2-Ni cermets, Ceram. Int. 43 (2017) 17202–17205, https://doi.org/10.1016/j.ceramint.2017.09.145.
[5] D.E. Cooper, N. Blundell, S. Maggs, G.J. Gibbons, Additive layer manufacture of Inconel 625 metal matrix composites, reinforcement material evaluation, J. Mater. Process. Technol. 213 (2013) 2191–2200, https://doi.org/10.1016/j.jmatprotec.2013.06.021.
[6] W.Y. Zhai, Y.M. Gao, Z.F. Huang, L. He, Cr3C2–20% Ni cermets prepared by high energy milling and reactive sintering, and their mechanical properties, Adv. Appl. Ceram. 115 (2016) 327–332, https://doi.org/10.1080/17436753.2016.1149908.
[7] J. Pirso, M. Viljus, S. Letunovits, K. Juhani, Reactive carburizing sintering—a novel production method for high quality chromium carbide–nickel cermets, Int. J. Refract. Met. Hard Mater. 24 (2006) 263–270, https://doi.org/10.1016/j.ijrmhm.2005.06.002.
[8] M. Sundararaman, P. Mukhopadhyay, S. Banerjee, Carbide precipitation in nickel base superalloys 718 and 625 and their effect on mechanical properties, TMS Superalloys 718 (1997) 625–706, https://doi.org/10.7449/1997/Superalloys_1997_367_378.
[9] B. Matović, T. Yano, Silicon Carbide and Other Carbides: From Stars to the Advanced Ceramics, Handb. Adv. Ceram. Mater. Appl. Process. Prop. Second Ed. (2013) 225–244. doi: 10.1016/B978-0-12-385469-8.00014-9.
[10] H. Zhang, X. Dong, S. Chen, Solid particle erosion-wear behaviour of Cr3C2–NiCr coating on Ni-based superalloy, Adv. Mech. Eng. 9 (2017), https://doi.org/10.1177/1687814017694580, 168781401769458.
[11] D. Verdi, C.J. Múnez, M.A. Garrido, P. Poza, Process parameter selection for Inconel 625-Cr3C2 laser cladded coatings, Int. J. Adv. Manuf. Technol. 92 (2017) 3033–3042, https://doi.org/10.1007/s00170-017-0372-4.
[12] A. Özer, Y.K. Tür, Sintering behaviour and mechanical properties of Cr3C2–NiCr cermets, Bull. Mater. Sci. 36 (2013) 907–911, https://doi.org/10.1007/s12034-013-0541-5.
[13] S.S. Hwang, Y.S. Lim, S.W. Kim, D.J. Kim, H.P. Kim, Role of grain boundary carbides in cracking behavior of Ni base alloys, Nucl. Eng. Technol. 45 (2013) 73–80, https://doi.org/10.5516/NET.07.2012.013.
[14] E. Whitney, G. Smikovich, J. Fink, high temperature oxidation of a modified alloy 625, superalloys 718, 625, 706 Var. Deriv. (1997) 695–704. doi: 10.7449/1997/Superalloys_1997_695_704.
[15] W. Zhai, Y. Gao, L. Sun, L. He, Y. Wang, Improvement of high temperature oxidation behavior of Cr3C2-20 wt% Ni cermets by adding 1 wt% Mo, J. Alloys Compd. 731 (2018) 271–278, https://doi.org/10.1016/j.jallcom.2017.10.012.